Journal of Pathology
J Pathol 2010; **220**: 530–541
Published online 11 December 2009 in Wiley InterScience
(www.interscience.wiley.com) **DOI**: 10.1002/path.2671

Original Paper

The role of the polyol pathway in acute kidney injury caused by hindlimb ischaemia in mice

Soroku Yagihashi,[1]* Hiroki Mizukami,[1] Saori Ogasawara,[1] Shin-Ichiro Yamagishi,[1] Hitoshi Nukada,[2] Noriaki Kato,[3] Chihiro Hibi,[3] Sookja Chung[4] and Stephen Chung[5]

[1]*Department of Pathology and Molecular Medicine, Hirosaki University Graduate School of Medicine, Hirosaki, Japan*
[2]*Department of Medicine, University of Otago, Dunedin, New Zealand*
[3]*Department of Pharmacology, Sanwa Kagaku Kenkyusho, Nagoya, Japan*
[4]*Research Center of Heart, Brain, Hormone and Healthy Aging, and Department of Anatomy and Physiology, University of Hong-Kong, China*
[5]*Research Center of Heart, Brain, Hormone and Healthy Aging, and Department of Physiology, University of Hong-Kong, China*

*Correspondence to:
Dr Soroku Yagihashi,
Department of Pathology and Molecular Medicine, Hirosaki University Graduate School of Medicine, 5 Zaifu-cho, Hirosaki, Japan.
E-mail:
yagihasi@cc.hirosaki-u.ac.jp

No conflicts of interest were declared.

Received: 21 July 2009
Revised: 14 November 2009
Accepted: 7 December 2009

Abstract

The polyol pathway, a collateral glycolytic process, previously considered to be active in high glucose milieu, has recently been proposed to play a crucial role in ischaemia/reperfusion tissue injury. In this study, we explored the role of the polyol pathway in acute kidney injury (AKI), a life-threatening condition, caused by hindlimb ischaemia, and determined if inhibition of the polyol pathway by aldose reductase (AR) inhibitor is beneficial for this serious disorder. Mice 8 weeks of age rendered hindlimb ischaemic for 3 h by the clipping of major supporting arteries revealed marked muscle necrosis with accumulation of sorbitol and fructose in ischaemic muscles. Serum concentrations of blood urea nitrogen (BUN), creatinine phosphokinase (CPK), creatinine, tumour necrosis factor (TNF)-α as well as interleukin (IL)-6 were all elevated in these mice. Treatment with AR inhibitor (ARI) effectively suppressed muscle necrosis and accompanying inflammatory reactions and prevented renal failure. Similar to ARI-treated mice, AR-deficient mice were protected from severe ischaemic limb injury and renal failure, showing only modest muscle necrosis and significant suppression of serum markers of renal failure and inflammation. Thus, these findings suggest that the polyol pathway is implicated in AKI caused by ischaemic limb injury and that AR may be a potential therapeutic target for this condition.

Keywords: ischaemic hindlimb injury; polyol pathway; aldose reductase inhibitor; acute kidney injury

Introduction

With an increasing population of obese and diabetic patients, central and peripheral vascular diseases are now a worldwide problem, causing ischaemic tissue injury of the brain, heart, and many other vital organs, leading to life-threatening conditions [1,2]. Ischaemic limb injury is a typical complication of peripheral vascular diseases often accompanied by renal insufficiency, a condition called acute kidney injury (AKI) caused by remote organ damage [3,4]. An increasing need for vascular reconstruction for acute arterial obstruction in patients with peripheral vascular diseases has called for special attention on the risk of AKI and its prevention and effective treatment [3,4]. Although the mechanisms of how AKI develops after remote organ damage are now extensively explored, its pathogenesis still remains unclear [5,6].

The polyol pathway is a collateral glycolytic pathway from glucose to sorbitol and from sorbitol to fructose [7,8]. Aldose reductase (AR) is a key regulating enzyme converting glucose to sorbitol using NADPH as a coenzyme, and sorbitol dehydrogenase mediates the conversion from sorbitol to fructose. This pathway has been extensively investigated in the field of diabetes complications [7,8]. Increased polyol pathway with excessive consumption of NADPH results in decreased production of nitric oxide (NO) and reduced glutathione [8]. Reduction of NO and glutathione in turn causes ischaemia and vessel hyperpermeability, as well as increased free radical production. Such processes are now believed to operate in the development of diabetic complications [8,9].

Recently, it has been shown that the polyol pathway is activated under normoglycaemic conditions when tissues are exposed to ischaemia/hypoxia [10]. With the reduction of intracellular oxygen, glucose uptake is accelerated and impairment of mitochondrial function due to the reduced oxygen supply duly

activates the collateral glycolytic pathway [11,12]. Similar to hyperglycaemic conditions, activation of the polyol pathway caused by ischaemia/hypoxia results in cellular dysfunction and death associated with increased oxidative stress [11,12]. With this background, an experimental approach using an AR inhibitor (ARI) has been shown to be beneficial for ischaemic heart [12,13], brain [14], and retina [15]. However, it is still unknown whether this is also the case in ischaemic limb injury accompanied by AKI.

Materials and methods

Animals

Normal male C57BL/6J mice 8–12 weeks of age were used. They were subjected to right hindlimb ischaemia by the clipping of major supporting arteries as described below. To test the inhibitory effects of the ARI, groups of animals were pretreated with an ARI (fidarestat, 30 mg/kg per day) (Sanwa Kagaku Kenkyusho) orally for a week prior to ischaemic operation. Other animals were treated orally with the ARI (fidarestat, 30 mg/kg) once, 30 min or 1 h after the onset of ischaemia. At 24 h after the release of clipping, all the animals were anaesthetized with ether and blood was withdrawn from the right atrium. Blood chemistry was examined for blood urea nitrogen (BUN), creatinine, creatinine phosphokinase (CPK), and potassium by an autoanalyser (SpotChem EZ, SP-4430, Arkray, Kyoto, Japan). Serum cytokine levels of tumour necrosis factor (TNF)-α and interleukin (IL)-6 were examined by ELISA (Pierce Biotechnol, Inc, Rockford, IL, USA). The muscles and kidneys were then excised for biochemical and histological examinations.

To investigate the role of AR further, we used AR-knockout (AR-KO) mice for ischaemic hindlimb injury. Age-matched wild-type mice of the C57BL/6N strain were used as controls. The production of AR-KO mice has been reported previously [14,16] and the mice have been back-crossed to the C57BL/6N strain for 11 generations (N11).

All the animals used were male mice and were housed under diurnal lighting conditions and allowed access to food and water *ad libitum*. The protocol of this study was reviewed and approved by the Ethical Committee on the Use of Live Animals at Hirosaki University School of Medicine (Approval No 80–2000).

Induction of limb ischaemia

The methods for inducing ischaemic injury and the clinical characteristics of the current ischaemic model have been reported in detail previously [17,18]. Mice were anaesthetized with isoflurane and placed on a heating pad. Major arteries supplying the right hindlimb (abdominal aorta, right common iliac, femoral, and superficial circumflex iliac arteries) were occluded by microvascular clips (TSK-1, 40 g; Kyowa, Tokyo, Japan). The duration of ischaemia was 180 min. Microvascular clips were released to allow reperfusion for 24 h until the mice were killed by cardiac blood withdrawal under ether anaesthesia. During this experiment, limb blood flow at the footpad was constantly monitored by laser Doppler flowmetry that confirmed loss of flow after clipping and regaining of reflow after the release of clipping (see Supporting information, Supplemental data #1).

AR expression, tissue carbohydrate and glutathione concentrations in ischaemic muscle and kidney

For the detection of AR expression, muscle tissues as well as renal cortex and medulla from both control and AR-KO mice were homogenized in TSA (Tris-saline-acid)–PMSF (phenylmethylsulphonyl fluoride) buffer (pH 8.0) and centrifuged (15 000 rpm). SDS-PAGE was performed using the Xcell SureLock system (Invitrogen, San Diego, CA, USA) in the reducing condition. Aliquots of 100 mg samples of protein were dissolved in the same sample buffer [2.5% 2-mercaptoethanol, 62.5 mmol Tris–HCl, 10% glycerol, 2% SDS, 0.0025% bromophenol blue, and 50 mmol reducing agent (dithiothreitol; DTT), pH 6.8] and loaded onto the Novex Tris-glycine Pre-Cast Gel (Invitrogen). After completion of the migration, the proteins were transferred to a polyvinylidene fluoride membrane (Immobilon-P; Millipore, Bedford, MA, USA) in a transfer buffer (25 mmol Tris, 0.2 mol glycine, and 20% methanol) using a wet transfer unit of the Xcell SureLock system. The membrane was reacted with antibody to rat AR [19] and β-actin-specific antibody (Santa Cruz). A final incubation was carried out with peroxidase-conjugated anti-rabbit or anti-goat IgG (Santa Cruz) for 45 min at room temperature. Immunodetection was performed by enhanced chemiluminescence (Amersham-Pharmacia, Buckinghamshire, UK). To see the effects of ischaemia on AR expression, muscles made ischaemic were also examined.

For the measurement of tissue carbohydrate and glutathione concentrations, muscle tissues exposed to ischaemia were extirpated at the time of killing and immediately frozen and stored at −80 °C until the measurement. Renal cortical tissues were also subjected to the measurement of carbohydrate concentrations. Sorbitol and fructose contents in tissues were measured by liquid chromatography with tandem mass spectrometry (LC/MS/MS) methods described previously [20,21]. The concentrations were expressed as nanomoles per milligram per protein. Tissue glutathione concentrations were measured by a colorimetric assay kit (GSH-400TM assay; OxisRes, Portland, OR, USA).

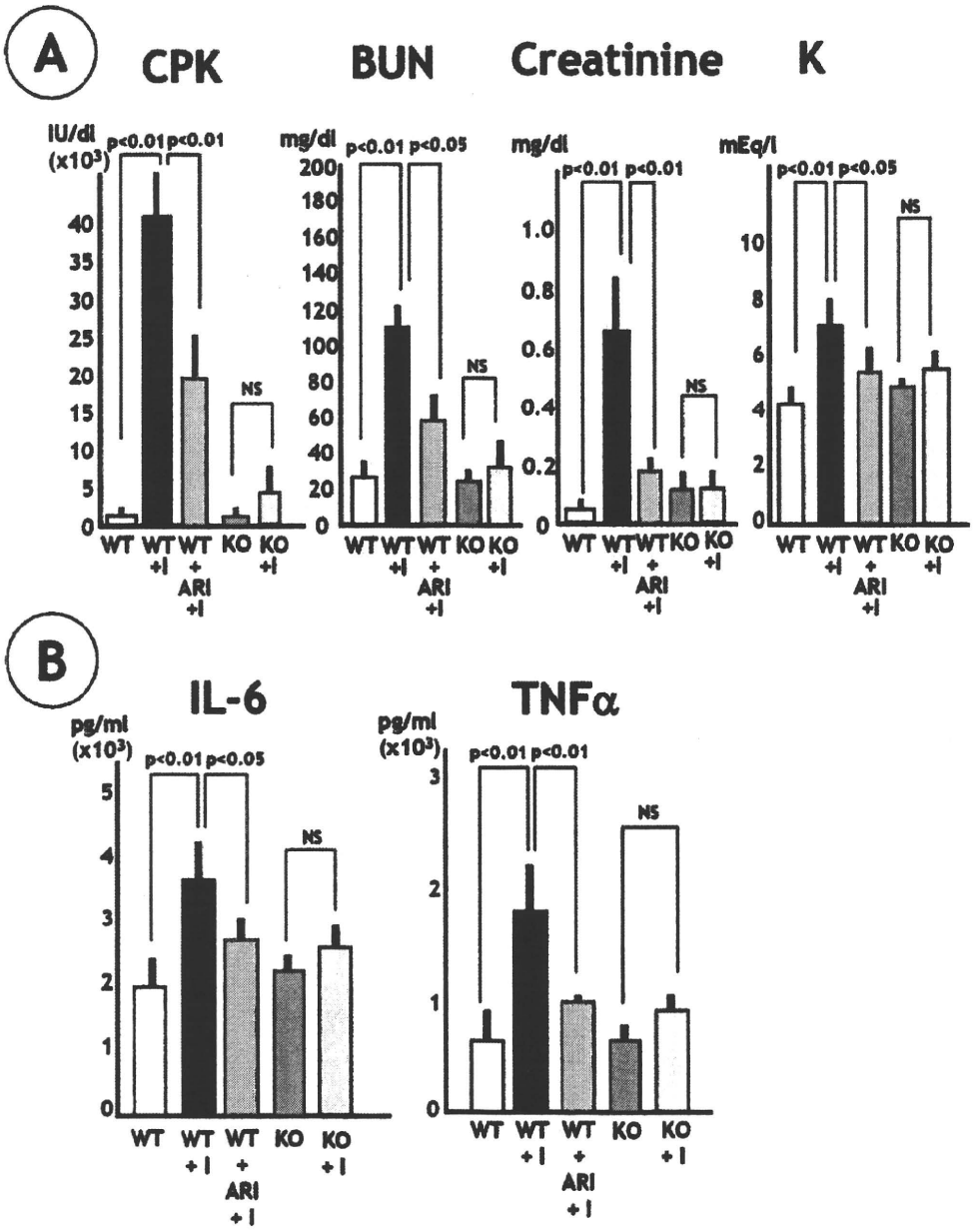

Figure 1. Laboratory data of experimental mice that developed hindlimb ischaemia and effects of pretreatment with the aldose reductase (AR) inhibitor and AR deficiency. (A) Serum markers of muscle damage and renal functions in experimental mice. Mice with hindlimb ischaemia (black bar; WT + I) showed elevated creatinine phosphokinase (CPK), blood urea nitrogen (BUN), creatinine, and potassium concentrations in the blood. These values were significantly suppressed in mice pretreated with the AR inhibitor (fidarestat) (WT + ARI + I). AR-KO mice (KO) did not show any elevation in these parameters and the values were not altered in AR-KO mice with hindlimb ischaemia (KO + I). (B) Serum cytokine levels in experimental mice. After limb ischaemia, serum interleukin-6 (IL-6) and tumour necrosis factor-α were significantly elevated in wild-type mice (WT + I). Treatment with the AR inhibitor suppressed the elevation of these values (WT + ARI + I). There was no significant elevation of these cytokines in AR-KO mice after limb ischaemia (KO + I) despite a trend for an increase

Histological evaluation and immunohistochemistry

The muscle and kidney tissues were fixed in 10% buffered formalin. After dehydration with ethanol, they were embedded in paraffin. Deparaffinized sections were rehydrated and stained with haematoxylin and eosin (H&E) for the evaluation of tissue changes and naphthol-ASD-chloroacetate-esterase (NACE) for the detection of neutrophils, respectively. To express the changes in an objective manner, myocytes undergoing coagulative necrosis were counted within a unit area of muscular tissues on H&E sections and expressed as number per unit muscle area. Neutrophils were also counted on NACE-stained slides and expressed as number per unit muscle area.

The kidney pathology was also examined on H&E and NACE-stained sections. Cortical areas were subjected to the evaluation of vacuolar degeneration of tubular cells. When more than 50% of tubular cells

J Pathol 2010; **220**: 530–541 DOI: 10.1002/path

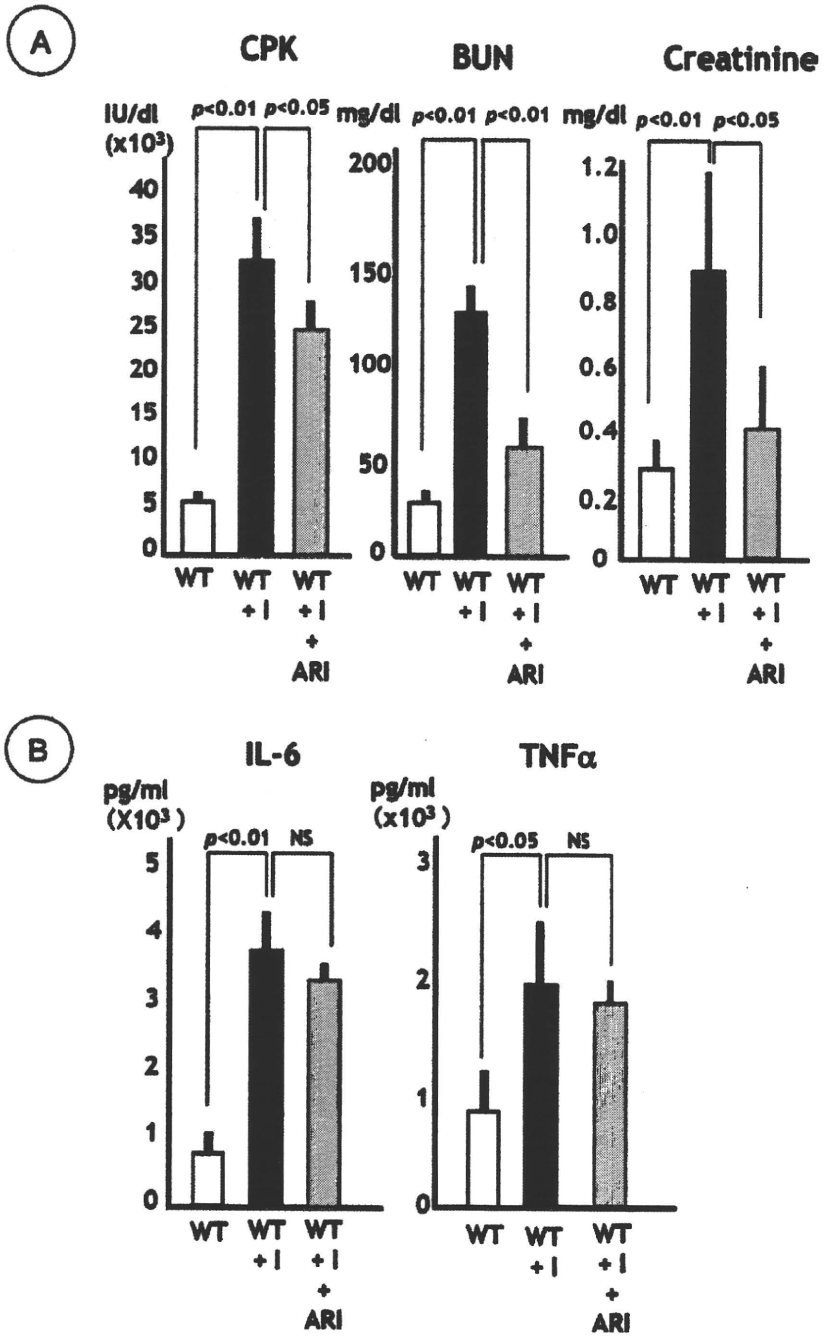

Figure 2. Laboratory data of experimental mice that developed hindlimb ischaemia and effects of delayed treatment with the aldose reductase (AR) inhibitor. (A) Effects of the AR inhibitor given 30 min after the onset of ischaemia on serum measures of muscle damage and renal function. Elevated concentrations of CPK, BUN, and creatinine were significantly suppressed in a group treated with ARI. (B) Effects of the AR inhibitor given 30 min after the onset of ischaemia on serum concentrations of cytokines. Elevated cytokine levels of IL-6 and TNF-α were not significantly affected by ARI treatment

were vacuolar, the change was scored as 3+; ≥20% to <50% of tubular cells, as moderate, 2+; ≥5% to <20%, as mild, 1+; and <5%, 0. Neutrophil counts were determined as number per unit area in cortex on NACE-stained sections.

Statistical analysis

All quantitative values are expressed as mean ± SE as a representative of a group. Statistical differences among groups were examined by analysis of variance with *post-hoc* Bonferroni corrections. p values less than 0.05 were considered to be significant.

Results

Laboratory data

After ischaemic injury, animals developed hindlimb paralysis and some died within 24 h due to acute

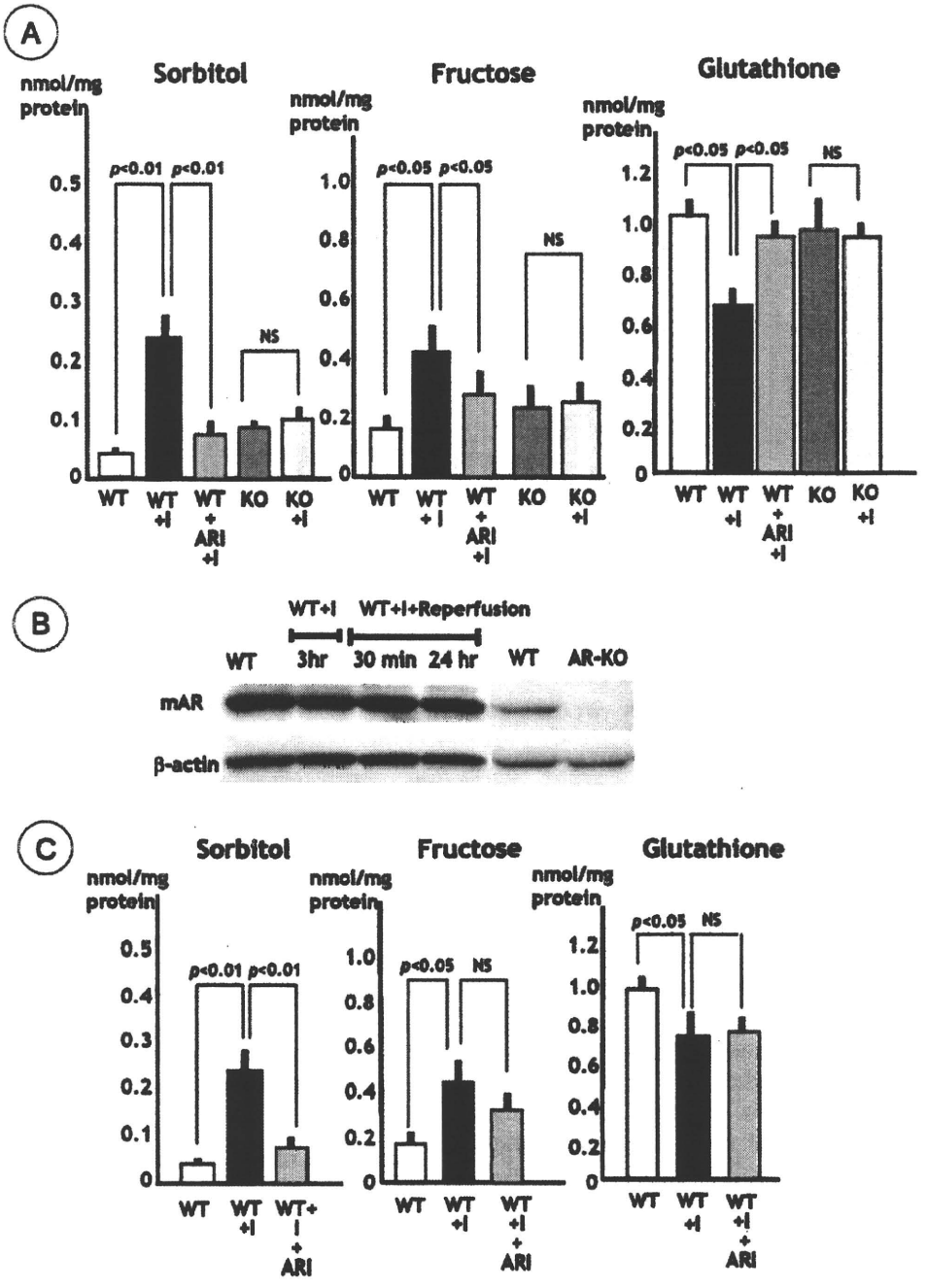

Figure 3. Carbohydrate and glutathione concentrations in muscles of experimental mice and AR expression. (A) After induction of ischaemia, there was marked accumulation of sorbitol and fructose in mice, of which the AR inhibitor significantly inhibited the accumulation. AR-KO mice did not respond to ischaemia and levels of sorbitol and fructose were not altered. With increased flux of polyol, tissue glutathione levels were significantly decreased in mice and ARI prevented the decrease. Glutathione levels of AR-KO mice were not affected by ischaemia. (B) Western blot analysis revealed expression of AR protein that was not influenced by ischaemia. As expected, there was no expression of AR in AR-KO mice. (C) Effects of the AR inhibitor started 30 min after the onset of ischaemia on polyol and glutathione concentrations in muscles of experimental mice. Reduced glutathione levels were not influenced by ARI treatment, although increased levels of sorbitol, but not fructose, were significantly suppressed

renal failure. They showed foot drop and poor movement of the right hindlimb. The paralysis gradually improved over the following 24 h in surviving animals. Untreated animals showed a high mortality rate of 53% (8/15), while animals pretreated with ARI for a week showed only modest impairment of leg movement and their mortality rate was 27% (4/15). Similarly, clinical behaviour in AR-KO mice after ischaemic injury was much milder than that in wild control mice. Only one out of 15 mice (7%) died after operation. The body weight and kidney weight were not differentially affected among the groups (data not shown).

Blood chemistry demonstrated significant increases in the concentrations of CPK, BUN, creatinine, and potassium in mice with ischaemic injury (Figure 1A).

J Pathol 2010; **220**: 530–541 DOI: 10.1002/path

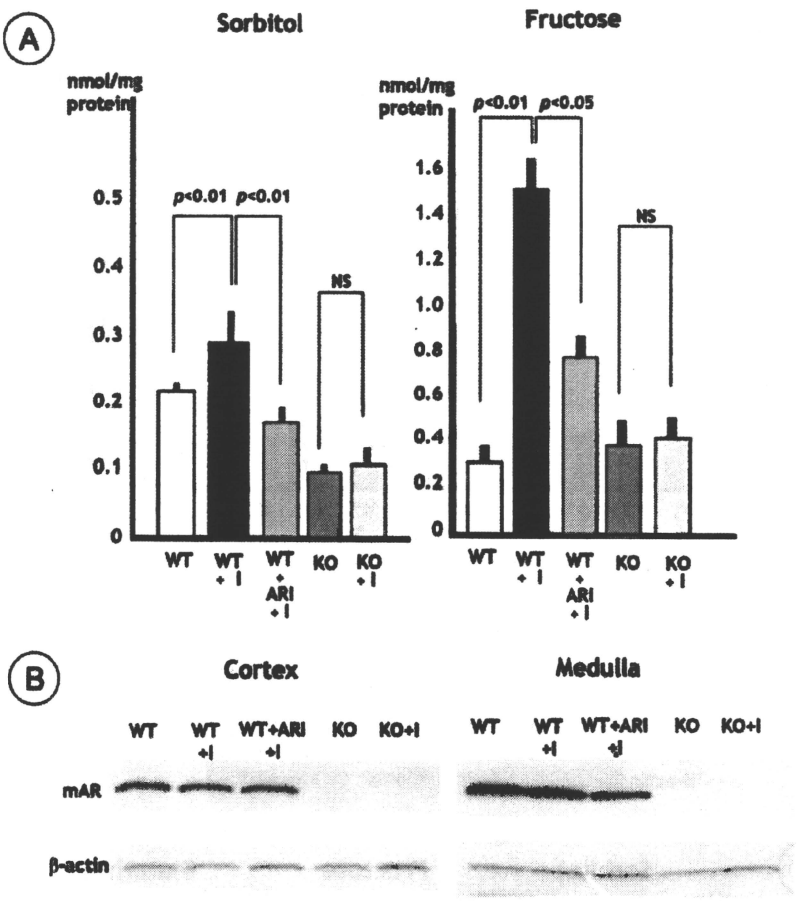

Figure 4. Carbohydrate levels in kidney cortex and AR expression in renal tissues in experimental mice. (A) There was significant elevation of sorbitol and fructose in mice with hindlimb ischaemia. Treatment with the AR inhibitor significantly inhibited the change. There was no alteration in AR-KO mice after ischaemia. (B) AR expression in renal cortex and medulla was comparable in experimental mice with or without hindlimb ischaemia. There was no expression in AR-KO mice

These values in ARI-pretreated animals were significantly lower, although higher than those in untreated animals. Concurrent with the data of ARI-treated mice, AR-deficient mice did not show a significant elevation of these measures. Serum cytokine levels of IL-6 and TNF-α were significantly increased in mice with ischaemic injury (Figure 1B). ARI treatment suppressed the rise of serum cytokines and there was no significant alteration in ischaemia-induced AR-KO mice. Animals with hindlimb ischaemia underwent marked oliguria or anuria and the effects of ARI were therefore not evaluated, although reduced urine creatinine concentrations were found in ARI-treated mice and AR-KO mice with hindlimb ischaemia (Supporting information, Supplemental data #2).

Mice treated with ARI 30 min after ischaemic injury also showed significant suppression of blood concentrations of BUN, CPK, and creatinine (Figure 2A). However, when ARI was given 1 h after the onset of ischaemia, there was no suppression of serum BUN, CPK, and creatinine (data not shown). In contrast, increases in the serum cytokine concentrations of IL-6 and TNF-α were not significantly affected by ARI administered either 30 min or 1 h after the onset of ischaemia (Figure 2B).

Polyol concentrations and AR expression in muscles and kidney

There was a marked accumulation of sorbitol and fructose in the calf muscles of mice exposed to ischaemia (Figure 3A). Glutathione concentrations were significantly suppressed in these mice. Pretreatment with ARI effectively prevented the rise of sorbitol and fructose, and the reduction of glutathione. In contrast, there was no significant alteration in the tissue concentrations of sorbitol, fructose or glutathione in AR-KO mice with or without ischaemic injury. Western blot analysis revealed that AR was expressed at a high level in muscles but its expression level was not affected in ischaemic muscles (Figure 3B). As expected, there was no AR expression in AR-KO mice.

When animals with ischaemia were treated with ARI 30 min after the injury, polyol products of sorbitol and fructose in the muscles were significantly smaller than those in untreated animals. However, reduced concentrations of glutathione were not significantly recovered by ARI treatment (Figure 3C).

Accumulations of sorbitol and, more prominently, fructose were markedly elevated in the renal cortex

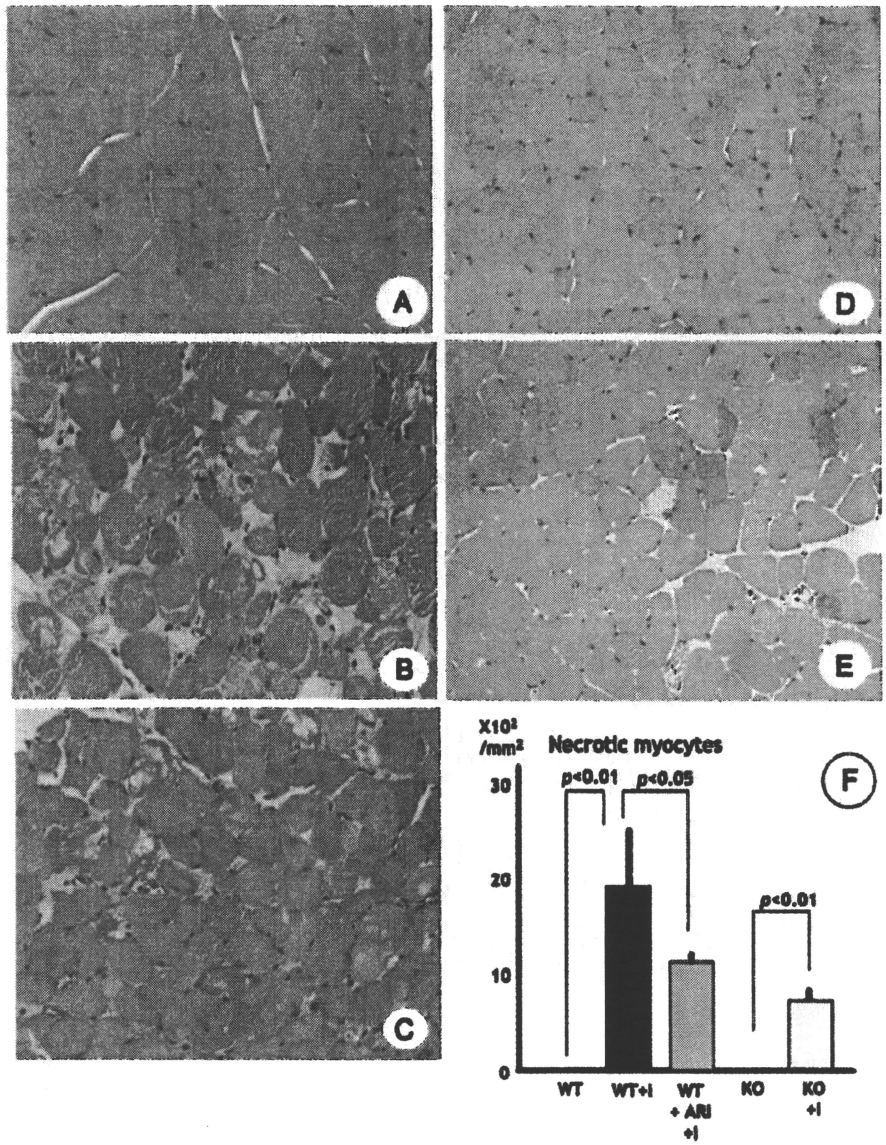

Figure 5. Muscle pathology in experimental mice. Non-treated mice showed intact features of striated myocytes (A). There were marked coagulative necrotic cells and vacuolations with inflammatory cells in mice with hindlimb ischaemia (B). Mice treated with ARI showed much milder pathological changes, with focal necrotic cells and modest inflammatory cells (C). On the other hand, muscles in AR-KO mice were intact (D) and hindlimb ischaemia caused modest coagulative degeneration and cell death of myocytes (E). Quantitation of necrotic myocytes demonstrated significant suppression in the appearance of necrotic cells in mice treated with ARI (F). AR-KO mice also showed a significant but modest increase in necrotic myocytes after hindlimb ischaemia

in mice with ischaemic hindlimbs, whereas ARI treatment inhibited this elevation significantly (Figure 4A). In AR-KO mice, there was no accumulation of sorbitol or fructose and ischaemic injury did not cause significant alterations. AR expression was not altered in either renal cortex or medulla in mice with hindlimb ischaemia, while AR deficiency was confirmed in AR-KO mice (Figure 4B).

Pathology of muscles and kidney

Muscle pathology

Hindlimb ischaemia caused marked necrosis of striated muscles in the calf and interstitial oedema associated with marked infiltration of neutrophils and mononuclear cells (Figure 5). Vacuolar degeneration as well as coagulative changes of myocytes was also noted. Mice pretreated with ARI showed less marked changes of muscle necrosis and degeneration. The muscles of ischaemia-induced AR-KO mice also showed only modest degeneration. There was marked infiltration of neutrophils in ARI-untreated mice with hindlimb ischaemia (Figure 6). ARI treatment before ischaemia markedly suppressed this change. Similarly, infiltration of neutrophils was not markedly increased in AR-KO mice even after ischaemic treatment. Quantitation of muscle lesions demonstrated a significant increase in necrotic cells and neutrophils in untreated ischaemic mice and ARI treatment suppressed these pathological changes. The changes in AR-KO mice

J Pathol 2010; **220**: 530–541 DOI: 10.1002/path

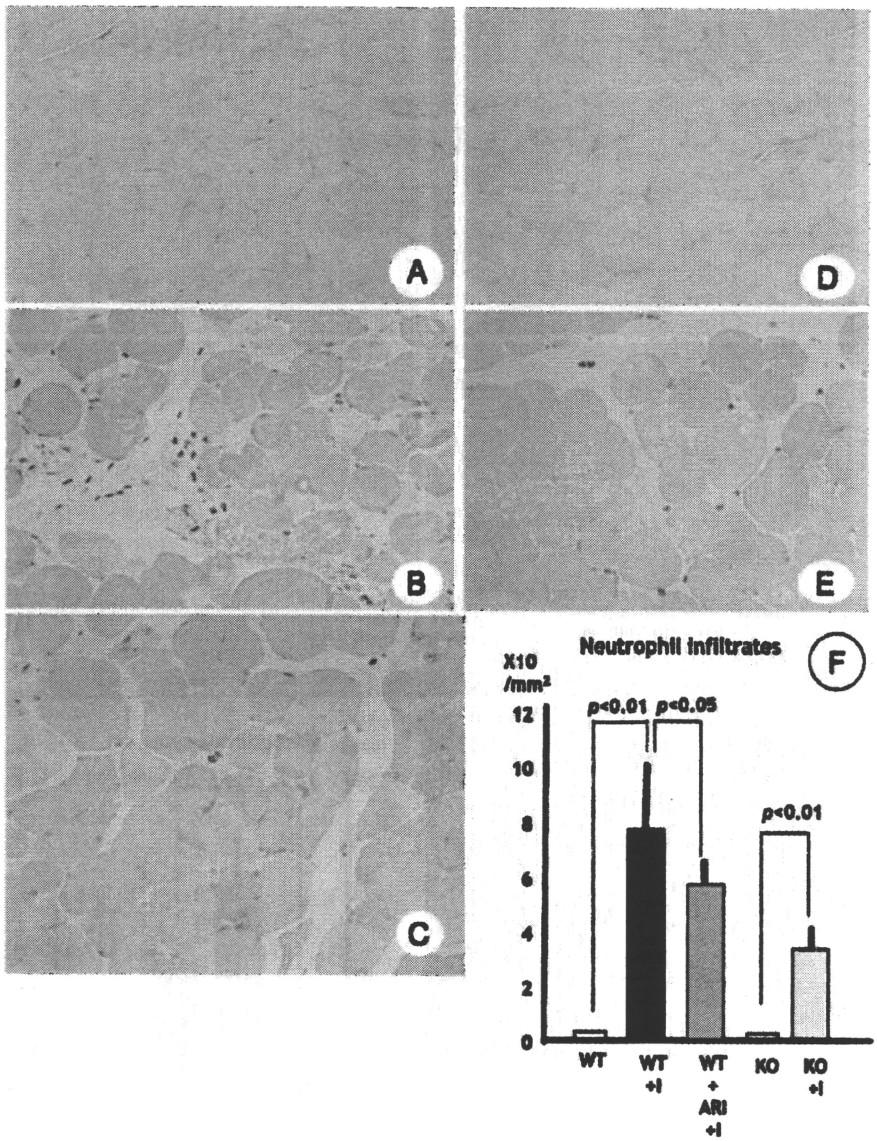

Figure 6. Neutrophilic infiltration of ischaemic hindlimb muscles (naphthol-ASD-chloracetate-esterase staining). There was no apparent infiltration of neutrophils in mice without ischaemia (A). Ischaemia caused severe infiltration of neutrophils (B) and this change was suppressed by ARI treatment (C). AR-KO mice did not show any pathological changes without ischaemia (D), whereas ischaemia caused only modest infiltration of neutrophils (E). Quantitation of neutrophil infiltration revealed a significant increase in the number of neutrophils in mice with hindlimb ischaemia and ARI treatment suppressed the infiltration of neutrophils (F). AR-KO mice also showed a modest increase in neutrophils after hindlimb ischaemia

were much milder than those in ischaemic control mice.

Kidney pathology

Mice that developed hindlimb injury showed renal failure. In these mice, renal tubular cells showed marked vacuolation and granular degeneration (Figure 7). ARI pretreatment significantly suppressed the degenerative changes of renal tubular cells. AR-KO mice did not show any marked degenerative changes in renal tubular cells after limb ischaemia. Similarly, after ischaemic limb injury, neutrophilic infiltration was noted in the interstitial area and within glomeruli (Figure 8). Mice treated with ARI showed less remarkable changes. Such changes of the tubular cells and neutrophilic infiltration were modest in ischaemia-induced AR-KO mice. Quantitation of renal tubular cell changes and neutrophilic infiltration supported the above findings.

Discussion

The present study first demonstrated that increased polyol pathway is implicated in acute kidney injury (AKI) elicited by ischaemic limb injury. Inhibition of this metabolic process with ARI significantly suppressed muscle injury and improved renal insufficiency. Implication of AR was further confirmed by the experiment in which AR-KO mice did not develop

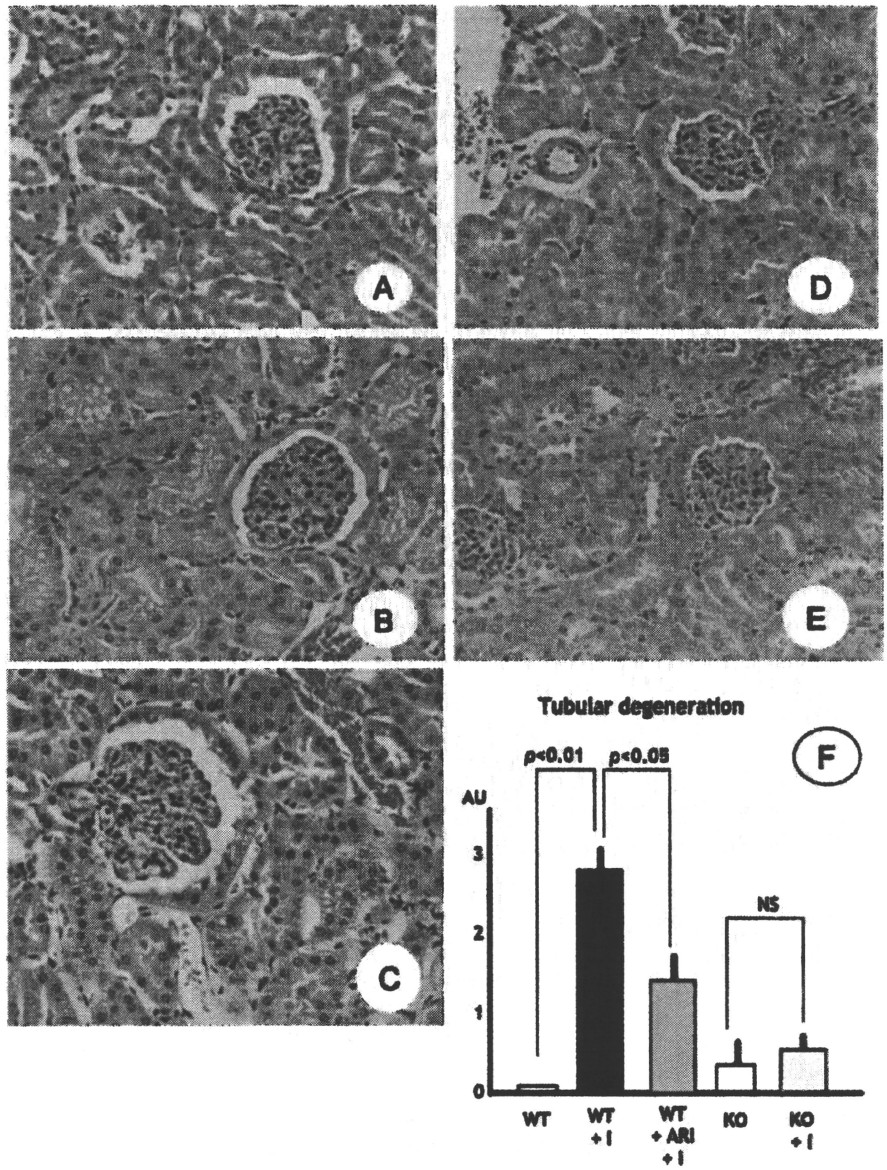

Figure 7. Kidney pathology in experimental mice. Compared with normal mice (A), tubular cells developed conspicuous vacuolar degenerative changes in mice with hindlimb ischaemia (B). ARI treatment markedly suppressed the change (C). AR-KO mice showed normal morphology (D) and only modest vacuolar changes after hindlimb ischaemia (E). Quantitation of cells with tubular degeneration revealed a significant increase in degenerated cells in mice with hindlimb ischaemia compared with control mice (F). Mice treated with the AR inhibitor showed a significant decrease in the frequency of degenerated cells. AR-KO mice showed only modest changes of tubular cell degeneration after hindlimb ischaemia ($p = 0.10$ versus KO)

AKI after hindlimb ischaemia. These novel findings indicate that an ARI may be beneficial for the treatment of ischaemic muscle injury with potential acute renal failure. This might also apply to similar clinical conditions such as ischaemia–reperfusion-induced hepato-renal syndrome [22,23] or traumatic crush syndrome [24,25]. The ARI effects were mediated not only by inhibition of sorbitol accumulation, but also possibly suppression of pro-inflammatory reactions as well as the improvement of other cellular signalling, most of which are well documented in the lesions of diabetic complications [8,9,21,26,27].

In this study, since the AR expression level was not altered in ischaemic muscles, the accumulation of polyol was mainly attributed to an increased flux of glucose. In fact, intracellular glucose uptake was increased in hypoxic conditions in either heart [28,29] or skeletal muscles [30], resulting in an increased flux of the polyol pathway [12,13]. With the reflow of oxygen, reactive radicals produce abundant aldehydes that are favoured substrates of AR, enhancing the activity of the polyol pathway [12,26,27]. As shown in *in vitro* studies, AR gene activation by TNFα and NO may also accelerate the polyol pathway flux [31,32]. Consequently, over-consumption of NADPH from the increased conversion of glucose to sorbitol may result in reduced synthesis of glutathione, yielding much free radical formation [26,27]. Such a vicious cycle may

J Pathol 2010; **220**: 530–541 DOI: 10.1002/path

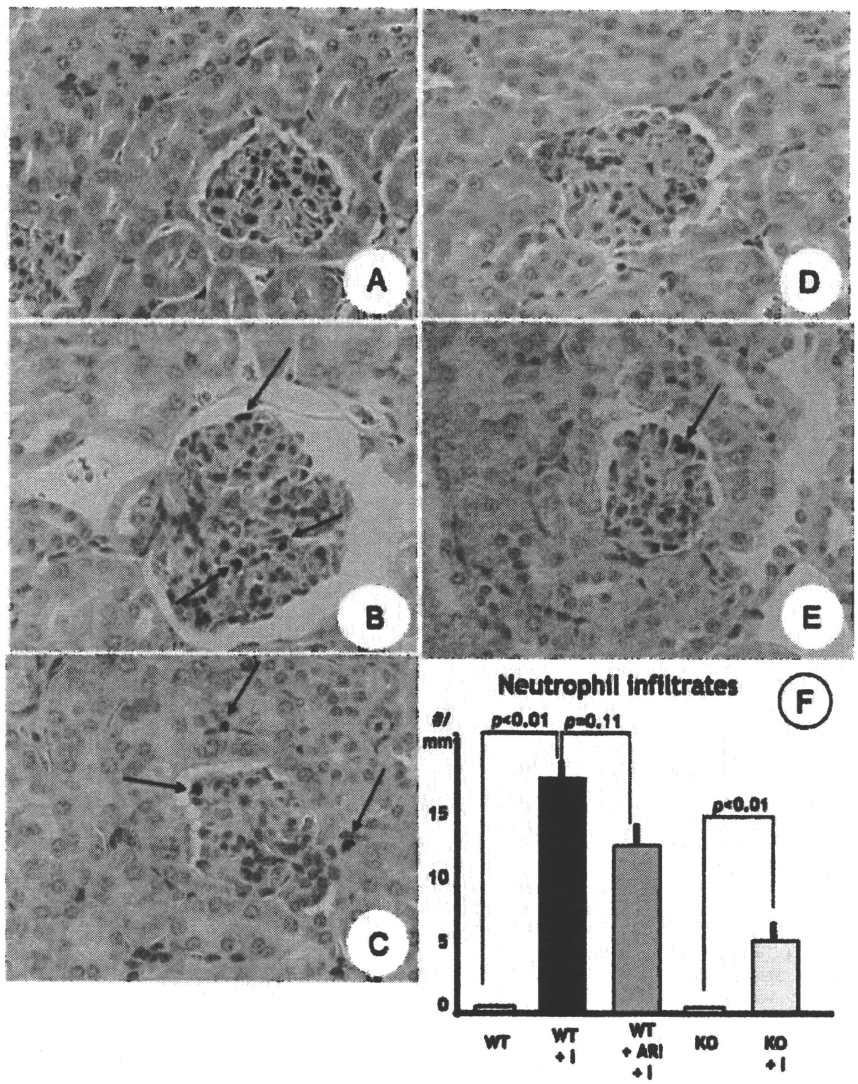

Figure 8. Neutrophilic infiltration of kidney in experimental mice (naphthol-ASD-chloracetate-esterase staining). There was no infiltration of neutrophils in mice without ischaemia (A). Ischaemia caused infiltration of neutrophils (arrows) in glomeruli and interstitium (B), and this change was equivocally suppressed by ARI treatment (C). AR-KO mice did not show apparent infiltration of neutrophils without ischaemia (D), whereas ischaemia caused only sparse infiltration of neutrophils (E). By quantitative analysis, there was a significant increase in neutrophils in mice with hindlimb ischaemia and mice treated with the AR inhibitor showed a trend for a decrease of neutrophils, although it was not significant ($p = 0.11$ versus untreated ischaemia-induced mice) (F). AR-KO mice with hindlimb ischaemia also showed an increase in neutrophils compared with untreated AR-KO mice

operate in tissues under ischaemia–reperfusion injury, but precise mechanisms are yet to be elucidated.

Involvement of the polyol pathway in ischaemia–reperfusion injury has been well documented in the heart [10,12,13], brain [14], and retina [15]. The effects of ARI on the tissue damage in these studies appear to be consistent with ours. Ischaemic necrosis of cardiac muscles was well prevented by ARI and transgenic mice overexpressing human AR showed augmented cardiac damage [12,13]. In an ischaemic heart, muscle damage was proposed to be mediated by an enhanced JAK/STAT pathway elicited by an altered NAD/NADH ratio caused by an increased flux of sorbitol to fructose [32,33]. The redox changes of NAD/NADH further induce PARP (polyADP-ribose polymerase) activation, leading to cell death [9,12,34]. In this setting, inhibition of sorbitol dehydrogenase was found to be effective in reducing the damage [33]. More recently, Lo *et al* reported that AR-KO mice were protected from ischaemic brain damage and that ARI treatment reduced the size of the infarcted area of the brain [14]. However, in their study, inhibition of sorbitol dehydrogenase did not suppress the brain damage [14]. Since we did not explore the redox changes or examine the effects of sorbitol dehydrogenase inhibitor, it remains to be determined whether the latter half of the polyol pathway or NAD/NADH alteration is meaningful in ischaemic limb injury and the accompanying renal failure in our model.

It is interesting to note that polyol products accumulated in renal cortical tissues in mice with AKI. ARI treatment inhibited renal cortical polyol accumulation and the damage of renal tubular cells. It has long been known that hindlimb ischaemia rapidly induces extreme renal cortical ischaemia since the historical documentation in a rabbit model by Trueta in 1947 (cited from ref 35). Hence, the rescue of renal failure in ARI-treated animals may well be accounted for by the suppressive effects of ARI on ischaemia-induced renal cortical damage. In addition, however, it should also be taken into account that renal failure in remote organ injury may be ascribed to activated cytokines [36], free radicals [37], or necrotic substances such as HMBG1 [38], released from damaged tissues. Neutrophils and their products are also implicated in AKI in ischaemia-induced hepatorenal syndrome [37,39,40]. In our study, the cytokine levels were well suppressed in ARI-treated mice but not in mice post-treated with ARI, in spite of the improvement of renal failure. This is in keeping with Kaneko et al's report that they could not find any reduction of cytokine levels in a group with ischaemic limb injury when treated with FGF2, although renal failure was ameliorated [6].

In our study, treatment with ARI before the application of ischaemic injury, similar to the AR-deficient conditions, was found to be effective, whereas ARI treatment after the onset of ischaemia was only partially effective. Serum concentrations of glutathione and cytokines were not suppressed in animals treated with ARI 30 min after the onset of ischaemia despite trends towards an improvement of renal failure. Hence, once the tissue injury is initiated, the immediate administration of ARI is essential to recover from the renal failure.

It has been shown that there is not much difference in life expectancy or clinical behaviour between untreated AR-KO and wild control mice, although AR deficiency causes diabetes insipidus-like conditions [16,41]. Nevertheless, AR-KO mice are known to be protective for neuropathy in diabetes [16]. The low mortality rate and less severe renal failure in ischaemic AR-KO mice found in this study may reinforce the implication of the polyol pathway in ischaemic–hypoxic tissue injury [8,11]. Exacerbation of ischaemic cardiac injury in mice overexpressing human AR accords with the notion that AR is an important determinant for the ischaemic renal injury and consequent renal failure [12,13]. AR was recently shown to be up-regulated more than twice in kidney grafts after transplantation and graft survival was improved with inhibition of this enzyme [42]. Following these recent findings, the current results may provide a new concept that increased polyol pathway after ischaemic injury is crucial for the tissue injury itself as well as subsequent induction of acute renal failure. The intervention of this process by ARI would be extremely useful for preventing such a life-threatening condition and worth clinical evaluation.

Acknowledgement

This study was supported by a grant-in-aid from the Ministry of Education, Science, Culture, and Sports, Japan (Nos 14370073 and 18659106) to S Yagihashi.

References

1. Ziegler D, Rathmann W, Dickhaus T, Meisinger C, Mielck A; KORA Study Group. Prevalence of polyneuropathy in pre-diabetes and diabetes is associated with abdominal obesity and macroangiopathy: the MONICA/KORA Augsburg Surveys S2 and S3. *Diabetes Care* 2008;**31**:464–469.
2. Sabouret P, Cacoub P, Dallongeville J, Krempf M, Mas JL, Pinel JF, *et al*. REACH: international prospective observational registry in patients at risk of atherothrombotic events. Results for the French arm at baseline and one year. *Arch Cardiovasc Dis* 2008;**101**:81–88.
3. Haimovici H. Muscular, renal, and metabolic complications of acute arterial occlusions: myonephropathic-metabolic syndrome. *Surgery* 1979;**85**:461–468.
4. Sakamoto S, Matsubara J, Matsubara T, Nagayoshi Y, Shono S, Nishizawa H, *et al*. Clinical effects of percutaneous cardiopulmonary support in severe heart failure: Early results and analysis of complications. *Ann Thorac Cardiovasc Surg* 2003;**9**:105–110.
5. Oue H, Sugimoto T, Okada M. Strategy of prevention of myonephropathic metabolic syndrome (MNMS): comparison of cooling and perfusion. *Kobe J Med Sci* 1999;**45**:13–25.
6. Kaneko K, Yonemitsu Y, Fujii T, Onimaru M, Jin C-H, Inoue M, *et al*. Free radical scavenger but not FGF-2-mediated angiogenic therapy rescues myonephropathic metabolic syndrome in severe hindlimb ischemia. *Am J Physiol Heart Circ Physiol* 2006;**290**:H1488–H1492.
7. Gabbay KH. Aldose reductase inhibition in the treatment of diabetic neuropathy: where are we in 2004? *Curr Diab Rep* 2004;**4**:405–408.
8. Chung SS, Chung SK. Aldose reductase in diabetic microvascular complications. *Curr Drug Targets* 2005;**6**:475–486.
9. Oates PJ. Aldose reductase, still a compelling target for diabetic neuropathy. *Curr Drug Targets* 2008;**9**:14–36.
10. Ramasamy R, Oates PJ, Schaefer S. Aldose reductase inhibition protects diabetic and nondiabetic rat hearts from ischemic injury. *Diabetes* 1997;**46**:292–300.
11. Ramasamy R, Trueblood N, Schaefer S. Metabolic effects of aldose reductase inhibition during low-flow ischemia and reperfusion. *Am J Physiol Heart Circ Physiol* 1998;**275**:H195–H203.
12. Hwang YC, Kaneko M, Bakr S, Liao H, Lu Y, Lewis ER, *et al*. Central role for aldose reductase pathway in myocardial ischemic injury. *FASEB J* 2004;**18**:1192–1199.
13. Iwata K, Matsuno K, Nishinaka T, Persson C, Yabe-Nishimura C. Aldose reductase inhibitors improve myocardial reperfusion injury in mice by a dual mechanism. *J Pharmacol Sci* 2006;**102**:37–46.
14. Lo ACY, Cheung A, Hung VKL, Yeung C-M, He Q-Y, Chiu J-F, *et al*. Deletion of aldose reductase leads to protection against cerebral ischemic injury. *J Cereb Blood Flow Metab* 2007;**27**:1496–1509.
15. Cheung AKH, Lo ACY, So KF, Chung SSM, Chung SK. Gene deletion and pharmacological inhibition of aldose reductase protect against retinal ischemic injury. *Exp Eye Res* 2007;**85**:608–616.
16. Ho EC, Lam KS, Chen YS, Yip JC, Arvindakshan M, Yamagishi S, *et al*. Aldose reductase-deficient mice are protected from delayed motor nerve conduction velocity, increased c-Jun NH2-terminal kinase activation, depletion of reduced glutathione, increased superoxide accumulation, and DNA damage. *Diabetes* 2006;**55**:1946–1953.
17. Nukada H, Powell H, Myers RR. Spatial distribution of nerve injury after occlusion of individual major vessels in rat sciatic nerves. *J Neuropathol Exp Neurol* 1993;**52**:452–459.
18. Baba M, Nukada H, McMorran D, Takahashi K, Wada R, Yagihashi S. Prolonged ischemic conduction failure after reperfusion in diabetic nerve. *Muscle Nerve* 2006;**33**:350–355.

19. Chakrabarti S, Sima AA, Nakajima T, Yagihashi S, Greene DA. Aldose reductase in the BB rat: isolation, immunological identification and localization in the retina and peripheral nerve. *Diabetologia* 1987;**30**:244–251.
20. Yamagishi S, Ogasawara S, Mizukami H, Yajima N, Wada R, Sugawara A, *et al.* Correction of protein kinase C activity and macrophage migration in peripheral nerve by pioglitazone, peroxisome proliferator activated-gamma-ligand, in insulin-deficient diabetic rats. *J Neurochem* 2008;**104**:491–499.
21. Uehara K, Yamagishi S, Otsuki S, Chin S, Yagihashi S. Effects of polyol pathway hyperactivity on protein kinase C activity, nociceptive peptide expression, and neuronal structure in dorsal root ganglia in diabetic mice. *Diabetes* 2004;**53**:3239–3247.
22. Arroyo V, Fernandes J, Gines P. Pathogenesis and treatment of hepatorenal syndrome. *Semin Liver Dis* 2008;**28**:81–95.
23. Najafi I, Van Biesen W, Sharifi A, Hoseini M, Farokhi FR, Sanadgol H, *et al.* Early detection of patients at high risk for acute kidney injury during disasters: development of a scoring system based on the Bam earthquake experience. *J Nephrol* 2008;**21**:776–782.
24. Kantarci G, Vanholder R, Tuglular S, Akin H, Koç M, Ozener C, *et al.* Acute renal failure due to crush syndrome during Marmara earthquake. *Am J Kidney Dis* 2002;**40**:682–689.
25. Chung KK, Perkins RM, Oliver JD 3rd. Renal replacement therapy in support of combat operations. *Crit Care Med* 2008;**36(7 Suppl)**:S365–S369.
26. Yabe-Nishimura C. Aldose reductase in glucose toxicity: a potential target for the prevention of diabetic complications. *Pharmacol Rev* 1998;**50**:21–33.
27. Srivastava SK, Ramana KV, Bhatnagar A. Role of aldose reductase and oxidative damage in diabetes and the consequent potential for therapeutic options. *Endocr Rev* 2005;**26**:380–392.
28. Russell RR 3rd, Li J, Coven DL, Pypaert M, Zechner C, Palmeri M, *et al.* AMP-activated protein kinase mediates ischemic glucose uptake and prevents postischemic cardiac dysfunction, apoptosis, and injury. *J Clin Invest* 2004;**114**:495–503.
29. Luptak I, Yan J, Cui L, Jain M, Liao R, Tian R. Long-term effects of increased glucose entry on mouse hearts during normal aging and ischemic stress. *Circulation* 2007;**116**:901–909.
30. Bosco G, Yang Z-I, Nandi J, Wang J, Chen C, Camporesi EM. Effect of hyperbaric oxygen on glucose, lactate, glycerol and anti-oxidant enzymes in the skeletal muscle of rats during ischemia and reperfusion. *Clin Exp Pharmacol Physiol* 2007;**34**:70–76.
31. Iwata T, Sato S, Jimenez J, McGowan M, Moroni M, Dey A, *et al.* Osmotic response element is required for the induction of aldose reductase by tumor necrosis factor-alpha. *J Biol Chem* 1999;**274**:7993–8001.
32. Kaiserova K, Srivastava S, Hetker JD, Awe SO, Tang XL, Cai J, *et al.* Redox activation of aldose reductase in the ischemic heart. *J Biol Chem* 2006;**281**:15110–15120.
33. Hwang YC, Shaw S, Kaneko M, Redd H, Marrero MB, Ramasamy R. Aldose reductase pathway mediates JAK-STAT signaling: a novel axis in myocardial injury. *FASEB J* 2005;**19**:795–797.
34. Obrosova IG, Pacher P, Szabo C, Zsengeller Z, Hirooka H, Stevens MJ, *et al.* Aldose reductase inhibition counteracts oxidative-nitrosative stress and poly(ADP-ribose) polymerase activation in tissue sites for diabetes complications. *Diabetes* 2005;**54**:234–242.
35. Better OS. Joseph Trueta (1897–1977): military surgeon and pioneer investigator of acute renal failure. *Am J Nephrol* 1999;**19**:343–345.
36. Liebethal W, Koh JS, Levine JS. Necrosis and apoptosis in acute renal failure. *Semin Nephrol* 1998;**18**:505–518.
37. Lee HT, Park SW, Kim M, D'Agati VD. Acute kidney injury after hepatic ischemia and reperfusion injury in mice. *Lab Invest* 2009;**89**:196–208.
38. Levy RM, Mollen KP, Prince JM, Kaczorowski DJ, Vallabhaneni R, Liu S, *et al.* Systemic inflammation and remote organ injury following trauma require HMGB1. *Am J Physiol Regul Integr Comp Physiol* 2007;**293**:R1538–R1544.
39. Klausner JM, Paterson IS, Goldman G, Kobzik L, Rodzen C, Lawrence R, *et al.* Postischemic renal injury is mediated by neutrophils and leukotrienes. *Am J Physiol* 1989;**256**:F794–F802.
40. Behrends M, Hirose R, Park YH, Tan V, Dang K, Xu F, *et al.* Remote renal injury following partial hepatic ischemia/reperfusion injury in rats. *J Gastrointest Surg* 2008;**12**:490–495.
41. Ho HT, Chung SK, Law JW, Ko BC, Tam SC, Brooks HL, *et al.* Aldose reductase-deficient mice develop nephrogenic diabetes insipidus. *Mol Cell Biol* 2000;**20**:5840–5846.
42. Gottmann U, Brinkkoetter PT, Hoeger S, Gutermann K, Coutinho ZM, Ruf T, *et al.* Atorvastatin donor pretreatment prevents ischemia/reperfusion injury in renal transplantation in rats: possible role for aldose-reductase inhibition. *Transplantation* 2007;**84**:755–762.

Supporting information on the internet

The following supporting information may be found in the online version of this article.

Supplementary data 1. Blood flow of footpad measured by laser Doppler flowmetry.

Supplementary data 2. Urine volume and urinary creatinine concentrations in experimental animals.

J Pathol 2010; **220**: 530–541 DOI: 10.1002/path

Neuropathy induced by exogenously administered advanced glycation end-products in rats

Yusuke Nishizawa[1], Ryu-ichi Wada[1], Masayuki Baba[2], Masayoshi Takeuchi[3], Chieko Hanyu-Itabashi[1], Soroku Yagihashi[1]*

ABSTRACT

Aims/Introduction: Advanced glycation end-products (AGE) have been implicated in the development of diabetic neuropathy. It still remains unknown, however, how AGE cause functional and structural changes of the peripheral nerve in diabetes. To explore the role of AGE in diabetic neuropathy, we examined the peripheral nerve by injecting AGE into normal Wistar rats.

Materials and Methods: Young, normal male Wistar rats were injected intraperitoneally (i.p.) daily for 12 weeks with purified AGE prepared by incubating D-glucose with bovine serum albumin (BSA). A control group received BSA alone. A group of rats given AGE were co-treated with aminoguanidine (50 mg/kg/day, i.p.). Peripheral nerve function and structure, as well as nerve Na^+,K^+-ATPase activity, were examined in these rats. Immunohistochemical expressions of 8-hydroxy-2′-deoxyguanosine (8OHdG) and nuclear factor-κB (NF-κB)p65 were also examined.

Results: Serum AGE levels were increased two to threefold in the AGE-treated group compared with those in the BSA-treated control group. AGE-treated rats showed a marked slowing of motor nerve conduction velocity (MNCV) and decreased nerve Na^+,K^+-ATPase activity compared with those in the BSA-treated group. These changes were accompanied by intensified expressions of 8OHdG and NF-κBp65 in endothelial cells and Schwann cells. Aminoguanidine treatment corrected MNCV delay, Na^+,K^+-ATPase activity, and suppressed the expression of 8OHdG and NF-κB, despite there being no influence on serum AGE levels.

Conclusions: The results suggest that an elevated concentration of blood AGE might be one of the contributing factors to the development of neuropathic changes in diabetes. (J Diabetes Invest, doi: 10.1111/j.2040-1124.2009.00002.x, 2010)

KEY WORDS: Advanced glycation end-products, Neuropathy, Oxidative stress

INTRODUCTION

Non-enzymatic glycation of structural proteins and the formation of advanced glycation end-products (AGE) have been implicated in the pathogenesis of diabetic complications[1,2]. The peripheral nervous system is one of the major targets for AGE-induced tissue damage. Human diabetic nerves exhibit an excessive deposition of AGE that correlates with the severity of pathological changes[3]. In addition to direct deleterious effects of AGE, biological reactions of AGE binding with their receptors for AGE (RAGE) exert tissue injury, resulting in characteristic complications in diabetes[1,4]. Recent studies disclosed that upregulated RAGE expression in diabetes contributes to nerve dysfunction and neuropathic symptoms[5,6]. While RAGE overexpression in diabetic mice accelerated the neuropathic changes[6], deletion of RAGE gene was found to protect the progression of neuropathy in long-term hyperglycemia[7], thus implicating the role of AGE/RAGE interaction in the peripheral nerve injury.

[1]Department of Pathology and Molecular Medicine, Graduate School of Medicine, Hirosaki University, Hirosaki, [2]Division of Neurology, Aomori Prefectural Hospital, Aomori, and [3]Department of Pathophysiological Science, Faculty of Pharmaceutical Sciences, Hokuriku University, Kanazawa, Japan

*Corresponding author. Soroku Yagihashi Tel.: +81-172-39-5025 Fax: +81-172-39-5026 E-mail address: yagihasi@cc.hirosaki-u.ac.jp

Received 1 September 2009; revised 27 September 2009; accepted 6 October 2009

Blood AGE concentrations are known to be elevated in diabetic patients[8,9]. Vlassara *et al.* showed that normal rats, when injected with exogenous AGE, developed pathological lesions of renal glomeruli or aortic walls, reminiscent of diabetic complications[10,11]. In fact, exposure of vessel tissues to AGE causes augmented expression of cell adhesion molecules and vascular endothelial growth factors (VEGF), as well as increased vascular permeability[11,12]. It is yet to be clear, however, if circulatory AGE indeed influence peripheral nerve function and structure, contributing to the establishment of neuropathy. In the present study, we examined if the elevation of circulating AGE in rats given exogenous AGE causes deleterious effects on peripheral nerve tissues and if the induced changes are similar to those described in diabetic neuropathy.

MATERIALS AND METHODS

Preparation of AGE-BSA

The method of AGE production and its purification was carried out according to the description given by Vlassara *et al*[10–12]. In brief, 1.6 g bovine serum albumin (BSA; Fraction V, Sigma, St. Louis, MO, USA) was dissolved together with 3.0 g D-glucose (Wako Chem, Osaka, Japan) in 10 mL of 0.5 M sodium phosphate buffer (pH 7.4). The solution was deoxygenated with nitrogen and sterilized by ultrafiltration (0.45 μm filter) and incubated at 37°C for 90 days under aseptic conditions.

After unincorporated sugar was removed by dialysis in 20 mM sodium phosphate buffer (pH 7.4) containing 0.15 M NaCl, glucose-modified high molecular weight materials were purified by Heparin-Sepharose CL-4B (Amersham Pharmacia, Uppala, Sweden) column chromatography and used as AGE-BSA. Endotoxin content in all samples was measured by Limulus amoebocyte lysate assay (E-toxate, Sigma) and found to be less than 0.2 ng/mL. The AGE-BSA showed absorption and fluorescent spectra identical to those reported previously (excitation 370 nm; emission 440 nm)[13]. Protein concentration was determined by the Bradford method using BSA as a standard[14].

Animal Studies

Four-week-old, male Wistar rats (160–180 g; Japan Clea, Osaka, Japan) were used. After a 1-week adaptation period, they were divided into four groups (8–10 animals in each group) and AGE was given by intraperitoneal (i.p.) injection for 12 weeks as follows: AGE-low group, 20 mg/kg/day of AGE; AGE-high group, 200 mg/kg/day; AGE + aminoguanidine (AG) group, 20 mg/kg/day of AGE + 50 mg/kg/day of AG i.p. (Wako Chem). For comparison, control rats received BSA alone (BSA group; 20 mg/kg/day BSA). Rats were monitored weekly for bodyweight and biweekly for blood glucose. Blood samples were obtained by tail snipping and fasting blood glucose concentrations were measured by a glucose-oxidase method (Toecho Super II, Kagawa, Japan). All animal experimentation followed the guidelines of Hirosaki University (approval number #M99023).

Tissue Preparation

Animals were killed under deep anesthesia with pentobarbital sodium (50 mg/kg bodyweight i.p., Abbot, Chicago, IL, USA) after 12 weeks of AGE injection by cardiac withdrawal of blood. Blood samples were used to determine AGE concentrations. Thereafter, sciatic nerve tissues were excised and processed for biochemical analysis for Na^+,K^+-ATPase activity, AGE content, and structural analysis of myelinated nerve fibers and endoneurial microvessels.

Measurement of AGE Concentration

For measurement of tissue AGE, peripheral nerve tissues were rinsed with phosphate buffered saline and finely minced with scissors. Lipids were extracted with acetone/chloroform (1:1) by shaking gently overnight at 4°C. Samples were then dried by vacuum centrifugation and resuspended in 0.2 M NaPO4 buffer (pH 7.4). After two rinses with methanol and distilled water, the samples were transferred to HEPES buffer (Gibco, Grand Island, NY, USA) with 0.01 M CaCl2 for 12 h. Then collagenase (type VII, Sigma) was added at a 1:100 (w/w) ratio and the mixture was incubated for 48 h at 37°C under mild shaking. One drop of toluene was added to maintain sterility. Digested samples were then centrifuged at 15 000 *g*, and clear supernatants were examined fluorometrically with a spectrophotometer (model 100-50; Hitachi, Tokyo, Japan) at specific excitation and

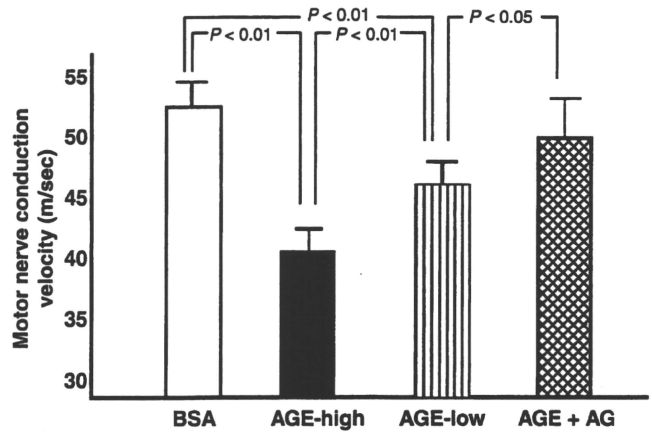

Figure 1 | The results of motor nerve conduction velocity (MNCV) in experimental animals. Compared with the levels of bovine serum albumin (BSA)-treated animals, both the advanced glycation end-products (AGE)-low (20 mg/kg/day) and the AGE-high (200 mg/kg/day) groups showed a significant delay. The aminoguanidine-treated group (AGE-AG) showed a significant improvement of MNCV. Each group consisted of 8–10 animals.

Table 1 | Laboratory data of experimental animals

Group	Number	Bodyweight (g)		Blood glucose (mmol/L)		AGE	
		Initial	End	Initial	End	Serum (AU/mL)	Nerve (AU/prot)
BSA	8	172 ± 54	318 ± 50	4.79 ± 0.29	4.61 ± 0.45	2.06 ± 0.37	0.13 ± 0.09
AGE-high	10	172 ± 63	329 ± 61	4.91 ± 0.39	4.78 ± 0.53	6.15 ± 1.25*,**	0.16 ± 0.12
AGE-low	8	164 ± 48	342 ± 43	4.91 ± 0.49	4.88 ± 0.88	4.33 ± 1.55*	0.14 ± 0.10
AGE-AG	8	163 ± 56	328 ± 54	4.80 ± 0.33	4.56 ± 0.64	5.32 ± 2.81*	0.14 ± 0.08

Values are mean ± SD. *P < 0.01 *vs* BSA group, **P < 0.05 *vs* AGE-low group. Serum AGE levels were measured by ELISA assay using specific antibodies against carboxymethyllysine. Nerve AGE levels were determined by the autofluorescence at the specific emission/excitation filters. AG, aminoguanidine; AGE, advanced glycation end-products; BSA, bovine serum albumin. AGE-high, rats treated with high-dose AGE (200 mg/kg) injection for 12 weeks. AGE-low, rats treated with low-dose AGE (20 mg/kg) injection for 12 weeks. AGE-AG, rats treated with low-dose AGE with aminoguanidine (50 mg/kg/day) for 12 weeks.

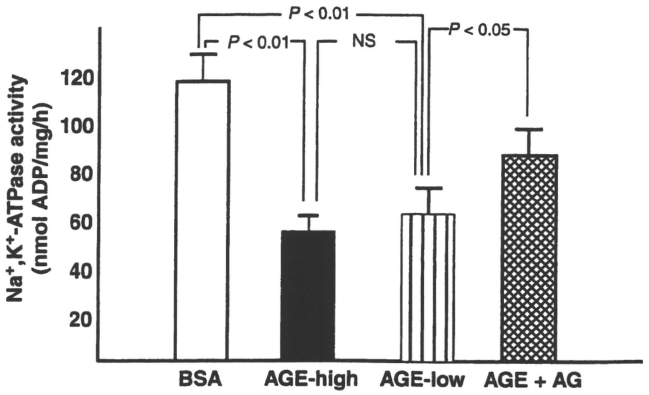

Figure 2 | Ouabain-sensitive Na^+,K^+-ATPase activity of the sciatic nerve in experimental rats. Na^+,K^+-ATPase activity was significantly reduced in the advanced glycation end-products (AGE)-low and the AGE-high groups compared with the bovine serum albumin (BSA)-treated group. The AGE-aminoguanidine (AG) group showed a slight but significant improvement of this enzyme activity. Each group consisted of eight animals.

emission 370/440 nm[15]. AGE was expressed by the intensity of fluorescence as arbitrary units per unit of protein content measured by the Bradford method[14].

Serum AGE levels were determined by a competitive enzyme-linked immunoassay (ELISA) using specific antibodies to carboxymethyllysine (CML) as described previously[8,12]. Briefly, test samples (50 μL) were added to each well as a competitor for 50 μL of AGE antiserum (1:2000) or purified antibodies (1:250–1:1500), followed by incubation for 2 h at room temperature with gentle shaking on a horizontal rotary shaker. Results were expressed as B/B0, calculated as (B/B0 = experimental OD − background OD)/(total OD − background OD). The immunoreactivity of each fraction was read from the calibration curve (CML-BSA) and was expressed as CML units (AU/mL), with 1U corresponding to the amount of antibody reactive material found in CML-BSA at a protein concentration of 1 μg/mL.

Measurement of Na^+,K^+-ATPase Activity

For measurement of Na^+,K^+-ATPase activity, sciatic nerves were excised and the perineurium was removed. The activity of Na^+,K^+-ATPase of ouabain-sensitive fraction was determined by the spectrophotometric enzymatic method as described[16].

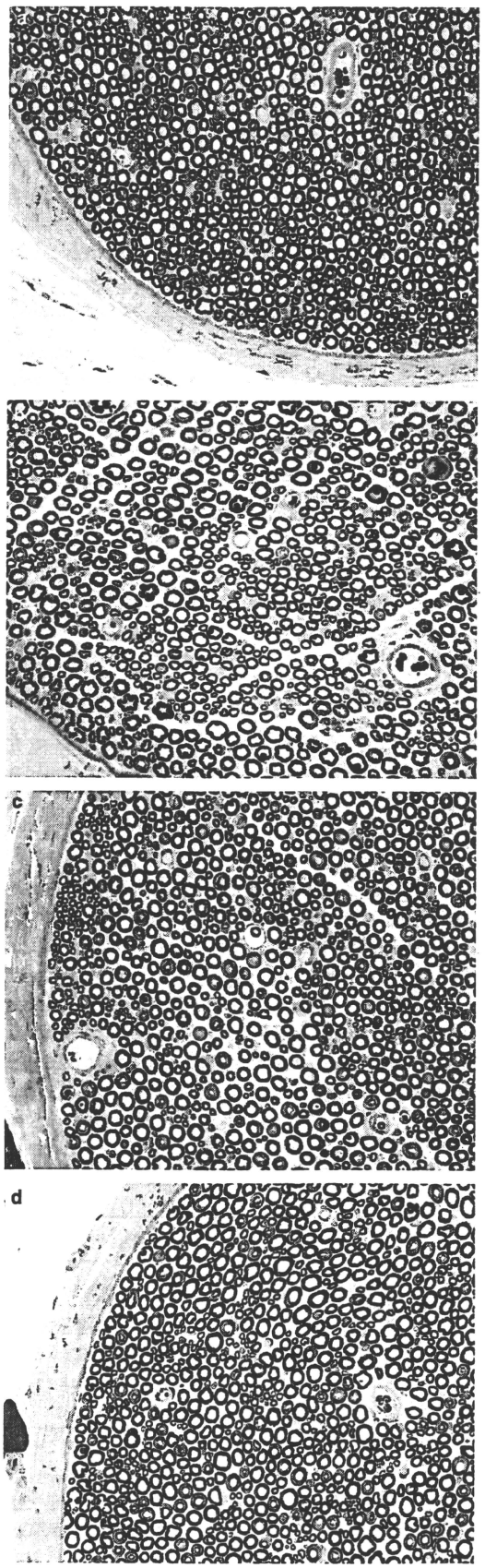

Figure 3 | Cross-sectional view of tibial nerves stained with toluidine blue in experimental animals. Compared with the sections from (a) bovine serum albumin (BSA)-treated animals, advanced glycation end-products (AGE)-treated animals showed interstitial edema (b, AGE-high; c, AGE-low). (d) Aminoguanidine treated group (AGE-AG) showed almost normal appearance.

Motor Nerve Conduction Velocity

Motor nerve conduction velocity (MNCV) was examined in all experimental animals. For these measurements, animals were anesthetized with ether. Body temperature was kept constant at 37°C on a thermostatically-controlled heating mat, and was continuously monitored with an anal temperature probe. Using a standard method, MNCV was measured in the left sciatic posterior tibial nerve using an evoked response stimulator (MS92 electromyogram device; Medelec, London, UK)[16,17].

Morphometric Analysis

At the end of the experiments, the right tibial nerves were excised and fixed overnight at 4°C in 2.5% glutaraldehyde buffered with 0.05 mmol/L sodium cacodylate (pH 7.3). The samples were then postfixed in 1% osmium tetroxide and dehydrated through an ascending series of ethanol concentrations. They were embedded in epon. One-micron thick semithin transverse nerve sections were stained with toluidine blue. For morphometric analysis, fascicular area, myelinated fiber density, myelinated fiber number, fiber size and fiber occupancy were measured at a magnification of ×2000 by a computer-assisted image analyzing system (NIH image, Version 1.6; NIH, Bethesda, MD, USA). The mean values of myelinated fiber size, measured as the area delineated by the outer myelin border, were calculated from at least 800 fibers randomly selected from 6–8 frames of each nerve fascicle. Fiber occupancy was calculated by dividing total fascicular area by the number of myelinated fiber × mean fiber size in each rat. Tissues affected by fixation artifacts were excluded from analysis.

To evaluate the changes of endoneurial microvessels, the number of capillaries in each tibial nerve fascicle was counted on semithin sections at a magnification of ×1000 and expressed as number of capillaries per unit area. For evaluation of endoneurial vascular changes, ultrathin sections were obtained with ultramicrotome and stained with uranyl acetate and lead citrate. They were examined by a JEOL 2000 electron microscope (Nihon Denshi, Tokyo, Japan). Five to eight microvessels were observed for the qualitative changes of endothelial cells and morphometric analysis of vessels. Vascular area size, endothelial cell area, luminal patency ratio relative to the whole vascular area and basement membrane thickness were measured as previously described[18].

Immunocytochemistry

A midportion of the sciatic nerve was fixed in 10% formalin overnight and embedded in paraffin. Four micron-thick sections were deparaffinized with xylene and processed for immunohistochemical evaluation of the expression of 8-hydroxy-2′-deoxyguanosine (8OHdG) and an activated form of nuclear factor-kappa B (p65) (NF-κBp65). Antibodies to 8OHdG (N45.1, mouse monoclonal; JICA, Nihon-Yushi, Shizuoka, Japan) and NF-κBp65 (rabbit polyclonal; Santa Cruz Biotechnology, San Francisco, CA, USA) were obtained commercially. Before the application of the primary antibody, deparaffinized

Table 2 | Morphometric analysis of myelinated fibers in tibial nerve of experimental animals

Group	*n*	Total fascicular area (mm^2)	Myelinated fiber density (#/mm^2)	Myelinated fiber number (#/fasc)	Mean fiber size (μm^2)	Index of circularity	Mean fiber occupancy (%)
BSA	6	0.19 ± 0.03	10 583 ± 1010	2047 ± 339	51.6 ± 2.8	0.88 ± 0.01	54.0 ± 5.2
AGE-high	6	0.20 ± 0.04	9619 ± 1350	1987 ± 602	46.8 ± 5.1	0.91 ± 0.03	44.8 ± 6.3*
AGE-low	6	0.17 ± 0.03	10 050 ± 1314	1674 ± 437	48.6 ± 5.6	0.89 ± 0.01	48.4 ± 5.1
AGE-AG	6	0.19 ± 0.03	11 160 ± 1006	2058 ± 199	47.2 ± 4.1	0.89 ± 0.00	52.4 ± 2.7

Values are mean ± SD. *$P < 0.01$ *vs* BSA group.

AG, aminoguanidine; AGE, advanced glycation end-products; BSA, bovine serum albumin. AGE-high, rats treated with high-dose AGE (200 mg/kg) injection for 12 weeks. AGE-low, rats treated with low-dose AGE (20 mg/kg) injection for 12 weeks. AGE-AG, rats treated with low-dose AGE with aminoguanidine (50 mg/kg/day) for 12 weeks.

Table 3 | Morphometric analysis of endoneurial microvessels in tibial nerve of experimental animals

Group	*n*	Vascular density (#/mm^2)	Average vascular area (μm^2)	Endothelial area (μm^2)	Luminal patency ratio	Basement membrane thickness (μm)	Vacuolar changes of endothelial cells	Vacuolar mitochondria
BSA	6	61.6 ± 4.7	230 ± 95	31.7 ± 16.3	0.43 ± 0.12	1.45 ± 0.70	0.87 ± 0.32	2.40 ± 1.46
AGE-high	6	60.7 ± 15.4	148 ± 11	24.0 ± 16.4	0.45 ± 0.07	1.36 ± 0.47	2.50 ± 0.81*	4.30 ± 2.27*
AGE-low	6	70.7 ± 23.5	181 ± 12	30.7 ± 21.4	0.50 ± 0.06	1.27 ± 0.54	1.71 ± 0.40*	2.75 ± 0.43
AGE-AG	6	74.1 ± 21.7	212 ± 34	34.9 ± 53.1	0.51 ± 0.04	1.32 ± 0.49	1.06 ± 0.28**	2.51 ± 0.75

Values are mean ± SD. *$P < 0.01$ *vs* BSA group, **$P < 0.05$ *vs* AGE-low group.

AG, aminoguanidine; AGE, advanced glycation end-products; BSA, bovine serum albumin. AGE-high, rats treated with high-dose AGE (200 mg/kg) injection for 12 weeks. AGE-low, rats treated with low-dose AGE (20 mg/kg) injection for 12 weeks. AGE-AG, rats treated with low-dose AGE with aminoguanidine (50 mg/kg/day) for 12 weeks.

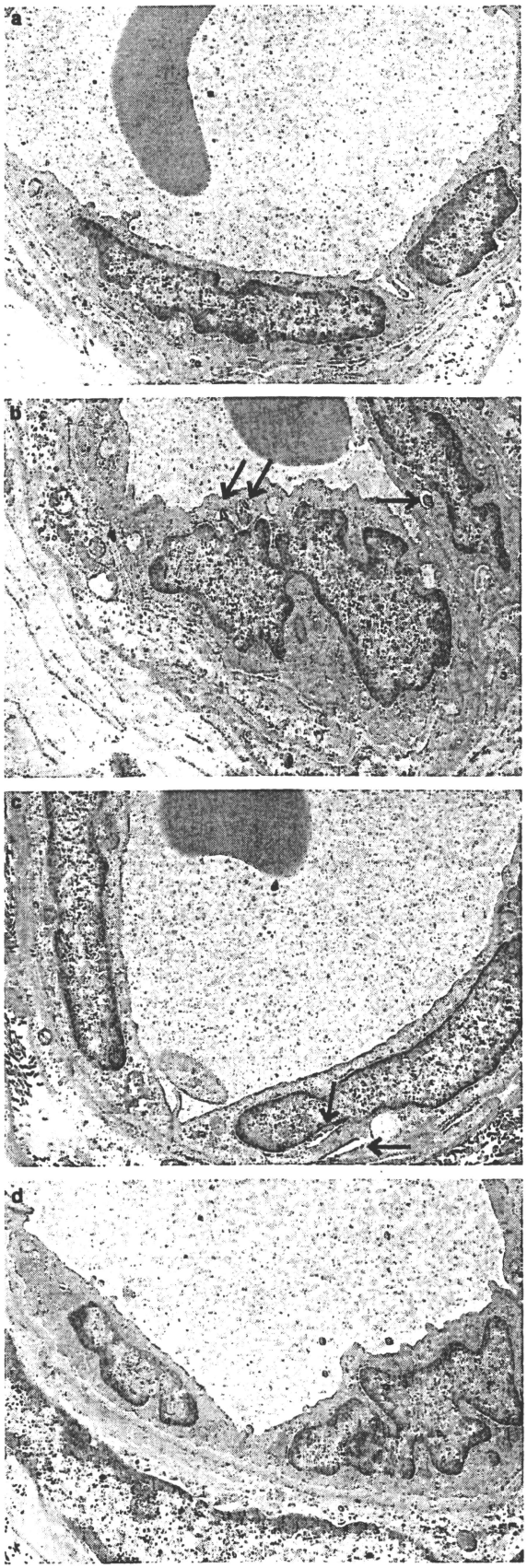

Figure 4 | Electron microscopic view of endothelial cells in experimental animals. (a) In normal rats, endothelial cells were flat, tightly adhered to neighboring cells. The endothelial cells in advanced glycation end-products (AGE)-treated animals (b, AGE-high and c, AGE-low) were swollen (double arrows) and contained many vacuolated bodies derived from mitochondria (arrow). (d) These changes were less prominent in aminoguanidine-treated animals (original magnification ×8000).

sections were pretreated with microwave irradiation (Milestone Srl., Sorrisole, Italy) for 3 × 5 times in citrate buffer for antigen retrieval. Antibodies to 8OHdG and NF-κBp65 were then applied to the sections overnight at 4°C. The sections were then incubated with secondary biotinylated antibody and streptavidin-biotin reagent (Histofine SAB-PO kit; Nichirei, Tokyo, Japan). The antigen–antibody complex was visualized by 3,3′-diaminobenzidine. For the objective evaluation, four samples from each animal group were mounted on a single slide and stained under the same conditions. Clear nuclear positive reactions of 8OHdG and NF-κBp65 were identified as positive. The frequency of positive cells was expressed as a percentage of total nuclei. At least 200–350 cells were counted in each section. Tissue sections affected by artifacts were discarded for analysis.

Statistical Analysis

Results were expressed as mean ± SD. Comparisons were made using a one-way ANOVA, followed by post-hoc Bonferroni's corrections. Unpaired Student's *t*-test was used for the comparison between AGE-low and AGE-AG groups. Statistical significance was considered when *P*-values were <0.05.

RESULTS

Bodyweight and Blood Glucose Level

During the observation period, fasting blood glucose and mean bodyweight were not significantly different among all the groups (Table 1). No animals died during the experiment.

AGE Concentrations in Serum and Nerve

The mean AGE concentration as reflected by CML values in serum was 2.1 and 3.0-fold higher in the AGE-low and the AGE-high groups, respectively, compared with those in the BSA group ($P < 0.01$ for both). AG treatment did not significantly influence the values of AGE in the serum (Table 1). Tissue concentration of AGE in the sciatic nerve determined by autofluorescence did not differ among the groups.

Motor Nerve Conduction Velocity

At the end of the experiments, AGE-treated rats showed slowed motor nerve conduction velocity (MNCV; Figure 1). The AGE-low group showed 14% decrease in average MNCV compared with BSA-treated animals ($P < 0.01$). This decrease was further augmented to 26% in the AGE-high group ($P < 0.01$ *vs* both BSA group and AGE-low dose group). AG treatment significantly improved the slowed MNCV ($P < 0.05$ *vs* AGE-low group).

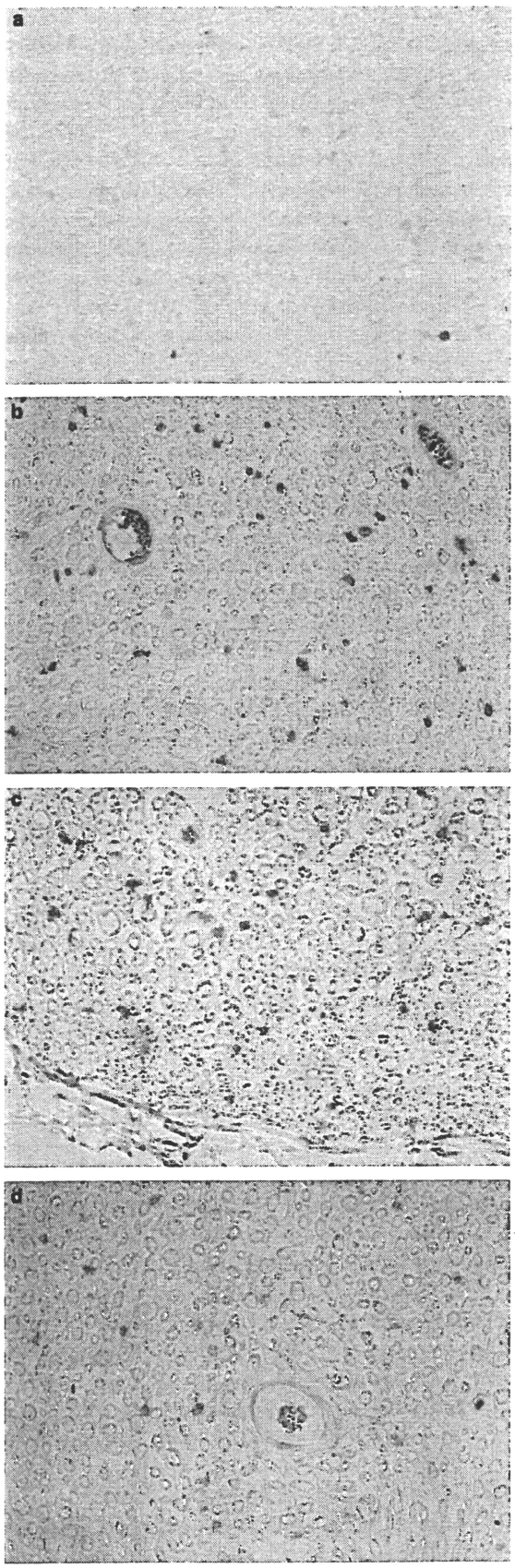

Figure 5 | Cross-sectional view of immunostained sections with 8-hydroxy-2′-deoxyguanosine (8OHdG). (a) There were only a few cells faintly stained in the bovine serum albumin (BSA)-treated group. By contrast, clear positive reactions were shown in the nuclei of endothelial cells and Schwann cells in (b) the advanced glycation end-products (AGE)-high and (c) the AGE-low group. (d) Aminoguanidine-treated group (AGE-AG) showed a reduction of cells with positive reactions.

Na^+,K^+-ATPase Activity

Ouabain-sensitive Na^+,K^+-ATPase activity in AGE-treated animals was significantly decreased (Figure 2). The AGE-high group showed 40% reduction ($P < 0.01$ *vs* BSA group) and the AGE-low group showed 33% reduction ($P < 0.01$ *vs* BSA group). There was no significant difference between the AGE-low and AGE-high groups' levels. AG treatment significantly improved this reduction by 60% ($P < 0.05$ *vs* AGE-low group).

Nerve Structure

On tibial nerve cross sections, AGE-treated animals showed interstitial edema (Figure 3). AG treatment appeared to prevent the edema (Figure 3). There was no significant difference, however, in mean total fascicular area, myelinated fiber density, myelinated fiber number and mean myelinated fiber size between AGE-treated animals and the controls, although there was a trend toward smaller values of average myelinated fiber size in the AGE-high group ($P = 0.10$, AGE-high *vs* BSA group) (Table 2). By contrast, the fiber occupancy was significantly reduced in the AGE-high group compared with the BSA group ($P < 0.05$), indicating the presence of endoneurial edema in the AGE-high group. The differences between the AGE-low group and the BSA group, or between the AGE-low group and the AG-treated group were not significant, although average values were decreased in the AGE-low group ($P = 0.09$, AGE-low *vs* BSA group; $P = 0.13$ AGE-low *vs* AGE + AG group).

Vascular density, mean vascular area, endothelial area, luminal patency rate and basement membrane thickness did not differ among the groups (Table 3). However, vacuolation of cytoplasm and mitochondria was frequently observed in the endoneurial microvessels in animals treated with AGE-high (Figure 4), and AG-treatment inhibited such changes (Figure 4 and Table 3).

Immunohistochemistry of 8 OHdG and NF-κB (p65)

Immunohistochemical staining showed clear evidence of oxidative stress related DNA injury in AGE-treated nerves showing positive nuclear reactions of 8OHdG (Figure 5). In the AGE-high group, positive reactions were found in the nuclei of endothelial cells of endoneurial microvessels and Schwann cells. The AGE-low group also showed scattered cells positive for 8OHdG. The expression of 8OHdG was significantly inhibited in AG-treated rats. Quantitation of positive cells confirmed these findings (Table 4). Positive reactions of NF-κBp65 in the nuclei

Table 4 | Quantitative analysis of positive reactions to 8-hydroxy-2'-deoxyguanosine and nuclear factor kappa-B in the sciatic nerve of experimental animals

Group	*n*	8-hydroxy-2'-deoxuguanosine (%)	Activated nuclear factor-κB (%)
BSA	6	3.4 ± 1.0	2.0 ± 0.6
AGE-high	8	23.5 ± 8.2***	7.5 ± 0.7*****
AGE-low	6	12.5 ± 2.8*	5.2 ± 0.6*
AGE-AG	6	2.8 ± 1.2**	1.8 ± 0.5******

Values are mean ± SD. *$P < 0.01$ *vs* BSA group, **$P < 0.01$ *vs* AGE-low group, ***$P < 0.05$ *vs* AGE-low group.
AG, aminoguanidine; AGE, advanced glycation end-products; BSA, bovine serum albumin. AGE-high, rats treated with high-dose AGE (200 mg/kg) injection for 12 weeks. AGE-low, rats treated with low-dose AGE (20 mg/kg) injection for 12 weeks. AGE-AG, rats treated with low-dose AGE with aminoguanidine (50 mg/kg/day) for 12 weeks.

were also detected in the AGE-treated groups more commonly than in the BSA group (Figure 6 and Table 4). AG treatment suppressed this reaction.

DISCUSSION

The current study showed that elevated systemic AGE concentrations caused functional, biochemical and structural changes in the peripheral nerves of rats. The features are comparable to the neuropathic changes encountered in diabetic animal models[19–21]. Because AGE accumulation was not detected in peripheral nerve tissues in AGE-injected animals, the above neuropathic changes are likely to be mediated not by direct AGE reactions on the nerve fibers, but by the exposure of microvessels to exogenous AGE, thus eliciting endoneurial ischemia and altered vascular permeability. Because endoneurial microvessels did not show significant morphometric changes comparable to those found in diabetes, such as basement membrane thickening or alterations of vascular lumina, it appears that functional alterations of microvessels precede structural changes without accumulation of tissue AGE. The findings are consistent with reports which described effects of exogenously administered AGE on renal glomeruli and aortic tissues, recapitulating diabetic glomerulosclerosis or atheroma plaque formation[10,11].

Elevation of serum AGE is not limited to diabetic patients, as it is also detected in uremic patients[23–25]. Acceleration of vascular injury or worsening of chronic complications in diabetic

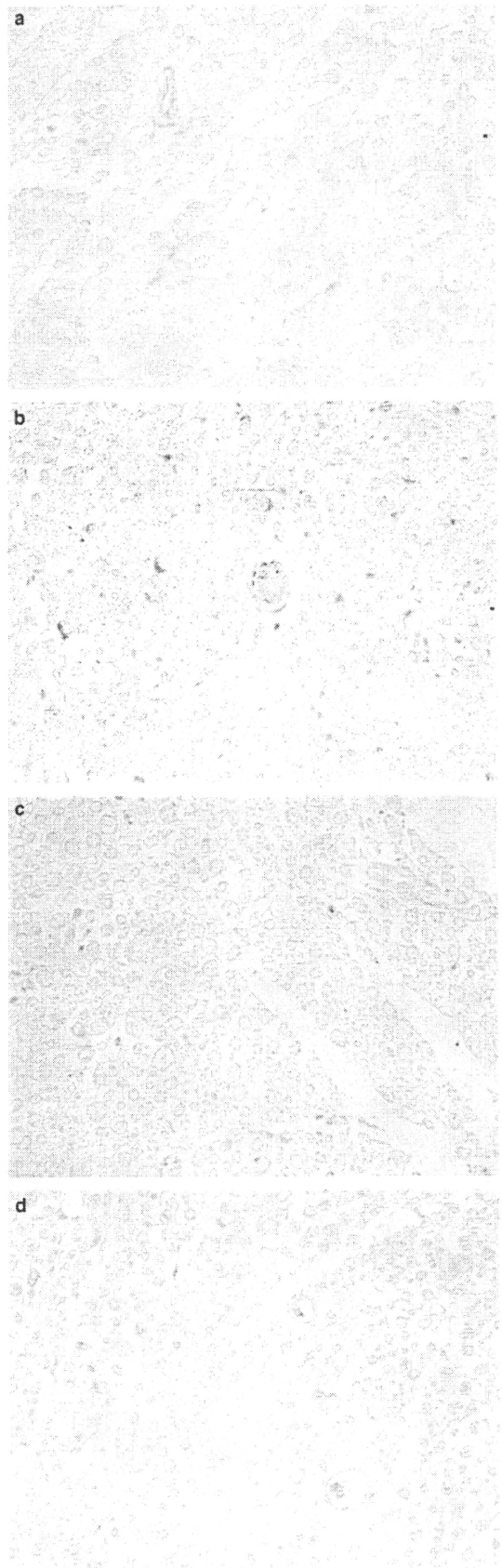

Figure 6 | Cross-sectional view of immunostained sections with nuclear factor-kappaB (NF-κB). (a) There was no clear positive reaction in the bovine serum albumin (BSA)-treated group. (b) By contrast, some nuclei of endothelial cells and Schwann cells in the advanced glycation end-products (AGE)-high group were definitely positive for NF-κB. (c) The reaction in the AGE-low group was equivocal. (d) Aminoguanidine-treated group (AGE-AG) did not show apparent positive reaction.

patients with uremia might be attributed not only to hyperglycemia but also to the toxic effects of AGE. The current findings further extend the contention that the severe delay in MNCV in uremic patients can be ascribed to elevated AGE concentrations in the blood[26,27]. The improvement of MNCV in uremic patients after dialysis of hemodiafiltration might be related to the decrease in AGE levels[28]. The dose-dependent severity of neuropathy in our AGE-injected animals might further indicate the importance of monitoring on the serum AGE concentration as a predictor for complications.

In the present study, we used BSA-derived AGE due to the availability of large amounts of AGE. One may wonder if the effects might be confounded by immunological reactions as a result of species difference. This is unlikely, because BSA-treated animals did not show apparent neuropathic changes. AGE constitute various chemical structures which show fluorescence or non-fluorescence. We confirmed that our AGE contained structures reactive to antibodies to both CML and non-CML, including imidazole or carboxyethyllysine (data not shown)[29]. Takeuchi *et al.* found that AGE derived from glyceraldehydes were toxic to neuronal cells and Schwann cells *in vitro*, causing apoptosis with activation of NF-κBp65, whereas CML did not show any deleterious effect[30,31]. It was also shown that glyceraldehyde-derived AGE have a strong affinity to RAGE[32]. Because we did not examine the effects of pretreatment with antibodies to specific components of AGE before injecting AGE, it was not possible to identify which component of AGE was the cause for neuropathic changes. Use of a specific type of AGE might clarify which component of AGE is most injurious to nerve tissues in future studies.

Most of the neuropathic changes we found in the present study might be accounted for by endoneurial vascular dysfunction caused by exogenous AGE. It has well been shown that neurovascular dysfunction is implicated in the early neuropathic changes in diabetic animal models[33–35]. In the diabetic condition, various metabolic cascades induced by hyperglycemia including polyol pathway, protein kinase C activity and oxidative stress as well as non-enzymatic glycation, all operate for the vascular impairment[33–35]. In the current study, we can assume that exposure of endothelial cells to AGE first exerts proinflammatory reactions of endoneurial vessels with enhanced expression of vasoactive substances, expression of cell adhesion molecules for leukocytes such as vascular cell adhesion molecule (VCAM) or intercellular cell adhesion molecule (ICAM), or secretion of cytokines such as tumor necrosis factor alpha (TNFα) or VEGF[22,36]. Oxidative stress is also generated after exposure of endothelial cells to AGE[37,38]. As a consequence, the nerve tissues might be followed by endoneurial ischemia with hyperpermeable milieu, resulting in reduced Na^+,K^+-ATPase activity and MNCV. This contention might be in part supported by a high expression of 8OHdG and NF-κBp65 in endothelial cells and Schwann cell nuclei detected in AGE-treated animals. The vacuolated cytoplasm and mitochondria frequently detected in AGE-treated animals might be in keeping with this view. Recent studies using RAGE transgenic mice showed that the levels of RAGE expression are important for the nerve tissue injury and sensory impairments through activation of NF-κBp65 in the diabetic condition[6,7].

In the present study, aminoguanidine effectively corrected MNCV and Na^+,K^+-ATPase activity. These effects are consistent with the results on the *in vivo* effects of AG or OPB 9195 on neuropathic changes in diabetic rats[15–17,39,40]. In these studies, tissue or serum AGE levels were significantly inhibited by treatment with these compounds, together with inhibition of 8OHdG expressions[15–17]. Interestingly, in the present study, we could not find any decrease of serum AGE in AG-treated animals, suggesting that the effects of AG were mediated by the inhibition of biological reactions of AGE/RAGE, thereby reducing oxidative stress and proinflammatory reactions. It should be cautioned, however, that aminoguanidine effects might also be ascribed to its direct inhibitory action of inducible NO synthase that can be induced by AGE[41].

In summary, the present study confirmed that AGE is a potent inciting factor for the development of neuropathy, and the inhibition of AGE/RAGE interaction might be a right target for the future treatment of diabetic neuropathy.

ACKNOWLEDGMENTS

The authors appreciate the excellent technical help of Yuko Sasaki, Nozomi Masuta and Kaori Okamoto during the study. This study was supported by grants from the Juvenile Diabetes Research Foundation International (#1-2000-263) and the Japanese Ministry of Education, Science, Sports and Culture (#10470054, #14370073). There is no conflict of interest in all the authors listed.

REFERENCES

1. Vlassara H. Recent progress on the biologic and clinical significance of advanced glycosylation end products. *J Lab Clin Med* 1994; 124: 19–30.
2. Brownlee M. Biochemistry and molecular cell biology of diabetic complications. *Nature Med* 2001; 414: 813–820.
3. Sugimoto K, Nishizawa Y, Horiuchi S, *et al.* Localization in human diabetic peripheral nerve of Nε-carboxymethyllysine-protein adducts, an advanced glycation endproduct. *Diabetologia* 1997; 40: 1380–1387.
4. Schmidt AM, Hori O, Chen JX, *et al.* Advanced glycation endproducts interacting with their endothelial receptor induce expression of vascular cell adhesion molecule-1 (VCAM-1) in cultured human endothelial cells and in mice. A potential mechanism for the accelerated vasculopathy of diabetes. *J Clin Invest* 1995; 96: 1395–1403.
5. Haslbeck KM, Schleicher E, Bierhaus A, *et al.* The AGE/RAGE/NF-κB pathway may contribute to the pathogenesis of polyneuropathy in impaired glucose tolerance (IGT). *Exp Clin Endocrinol Diabetes* 2005; 113: 288–291.
6. Bierhaus A, Haslbeck K-M, Humpert PM, *et al.* Loss of pain perception in diabetes is dependent on a receptor of

